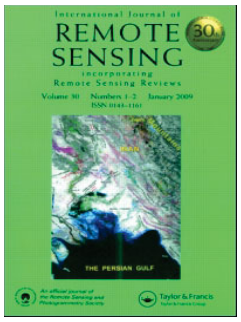

International Journal of Remote Sensing

ISSN: 0143-1161 (Print) 1366-5901 (Online) Journal homepage: http://china.tandfonline.com/loi/tres20

Colour balancing of satellite imagery based on a colour reference library

Lei Yu, Yongjun Zhang, Mingwei Sun & Xinyu Zhu

To cite this article: Lei Yu, Yongjun Zhang, Mingwei Sun & Xinyu Zhu (2016) Colour balancing of satellite imagery based on a colour reference library, International Journal of Remote Sensing, 37:24, 5763-5785, DOI: 10.1080/01431161.2016.1249306

To link to this article: http://dx.doi.org/10.1080/01431161.2016.1249306

Published online: 31 Oct 2016.

INTERNATIONAL JOURNAL OF REMOTE SENSING, 2016
VOL. 37, NO. 24, 5763–5785
http://dx.doi.org/10.1080/01431161.2016.1249306

Taylor & Francis
Taylor & Francis Group

Colour balancing of satellite imagery based on a colour reference library

Lei Yu, Yongjun Zhang, Mingwei Sun and Xinyu Zhu

School of Remote Sensing and Information Engineering, Wuhan University, Wuhan, Hubei, P.R. China

ABSTRACT

Generating mosaics of images obtained at different times is a challenging task because of the radiometric differences between the adjacent images introduced by the solar incident angle, atmosphere, and illumination condition. For most of the existing colour-balancing methods, the standard for determining the reference image is not unified, thus yielding different calibration results. Besides, traditional methods may suffer from colour error propagation and the two-body problems. A novel colour-balancing method for satellite imagery based on a colour reference library is proposed in this article, which aims to eliminate the effect of colour difference between different images for visually appealing and seamless image mosaicking. The proposed method contains two parts: the establishment of a colour reference library and the colour-balancing method based on it. Colour reference library is a database storing colour and other related information from the existing mosaic imagery. The colour information of the existing mosaic imagery is visually appealing and consistent with human visual perception. By automatically selecting appropriate colour reference information from the colour reference library according to the geographical scope and acquisition season information of the target images, the proposed approach provides effective solutions for choosing suitable reference image, colour error propagation, and the two-body problem in traditional colour-balancing methods. Experimental results demonstrate that the proposed approach performs well in the colour-balancing process.

ARTICLE HISTORY
Received 18 May 2016
Accepted 5 October 2016

1. Introduction

In the application of remote sensing, satellite imagery covering extensive areas such as regions, countries, or even whole continents (Cresson and Saint-Geours 2015) has become increasingly important (Olthof et al. 2005; Chen et al. 2014). Generally, the coverage of a single satellite image is limited due to the limitations of sensor design. Therefore, image mosaicking is usually adopted using images obtained at different times and even from different sensors to obtain images with large coverage. Influenced by factors such as solar incident angle, atmosphere, and illumination condition, colour differences exist between satellite images, which bring difficulty to image mosaicking

CONTACT Yongjun Zhang zhangyj@whu.edu.cn School of Remote Sensing and Information Engineering, Wuhan University, Wuhan, Hubei, P.R. China

(Chen, Vierling, and Deering 2005; Paolini et al. 2006; Liu et al. 2014). To eliminate the colour differences between images and obtain the seamless mosaic data, colour balancing (Xu and Mulligan 2010), also known as relative radiometric normalization (Chen, Vierling, and Deering 2005), was proposed and discussed.

Cresson and Saint-Geours (2015) concluded the purpose of remote-sensing image mosaicking into two aspects. The first purpose is quantitative, in which case further analysis of the mosaic image is needed to compute the thematic indices, such as vegetation or other quantitative products. Therefore, preservation of radiometric signal characteristics in a mosaic imagery is important, which means that the main objective is to ensure the radiometric fidelity of the mosaic. In this case, radiometric adjustment or radiometric normalization techniques are used. However, the second use of satellite image mosaics is qualitative, that is, to generate good-looking mosaics for illustrative use only. Such image mosaics should be visually appealing, seamless, and should reduce the technical issues related to satellite imagery acquisition. In this case, colour-balancing techniques are employed. In this article, we focus on a new colour-balancing technique to generate satellite image mosaics for illustrative use only.

There are numerous existing approaches of colour balancing, the majority of which designate a reference image for the image to be processed (hereinafter referred to as the target image) to adjust to (de Carvalho et al. 2013; Zhang, Wu, and Du 2014). These methods can be divided into non-linear correction and linear correction according to different adjustment approaches. The histogram matching method is the representation of the non-linear correction methods (Helmer and Ruefenacht 2005; Tsai and Huang 2005). Linear correction assumes that a linear transformation relationship in radiation information exists between the target image and the reference image (Moran et al. 1992; Song et al. 2001; Du, Teillet, and Cihlar 2002; Chen, Vierling, and Deering 2005; Sadeghi, Ebadi, and Ahmadi 2013), represented by statistics-based approaches such as Wallis transform (Sun and Zhang 2008), and methods based on invariant features such as iteratively reweighted Multivariate Alteration Detection (IR-MAD) (Canty and Nielsen 2008) and iterative slow feature analysis (I-SFA) (Zhang, Wu, and Du 2014).

Although these methods can eliminate colour differences between images to some extent, problems still exist. In cases of multi-temporal images covering the same area with small colour differences, the histogram matching approach is able to yield good results (Yang and Lo 2000). The Wallis transform method considers the image as a whole; as a result, the local colour characteristics of the image are ignored. The performance of the pseudo-invariant feature (PIF) method relies on the precision of invariant feature extraction, and the process is time consuming. Moreover, most of the available colour-balancing methods can only deal with a single pair of images at a time. Meanwhile, the normalization coefficients of an image may be affected by those of other images, which will easily result in the colour error propagation problem if there exists error in one of the colour normalization steps. The above conditions are called the two-body problem (Chen et al. 2014; Cresson and Saint-Geours 2015).

Besides the problems mentioned above, the selection of reference images is another key factor influencing the performance of the existing approaches (Ibrahim et al. 2015). However, the standard for determining the reference image is not unified. As illustrated by Canty and Nielsen (2008) and Cihlar et al. (2003), the reference image was considered the clearest target image, whereas the article by Chen et al. (2014) regarded it as the

image in the middle with the minimum distance to the other ones. Therefore, for the same group of target data, the reference images selected by different criteria may vary, thus yielding different calibration results.

According to the analysis above, the performance of the existing approaches is limited by the selection of the reference image besides principles. Therefore, it is an important problem to select the suitable reference image. Essentially, the role of the reference image is to provide reference colour information for colour-balancing methods. In the process of aerial triangulation, a library of control points is established to calculate the geographic coordinates of the image points (Wang et al. 2012). Similarly, it can be inferred that the principle above can be adopted to build a colour reference library providing reference colour information for colour-balancing methods, which has never been proposed before.

Under this condition, a novel colour-balancing method for image mosaicking based on the establishment of a colour reference library is proposed in this article. A colour reference library is a database where colour and other related information of the existing images is organized and stored under certain rules. The images that are selected to be stored in the colour reference library are the existing mosaic data sets or other images with the colour information that is visually appealing and consistent with the human visual perception. The advantages of the colour reference library are fully used in the proposed method by first selecting the suitable colour information as a reference and then building the pixel-to-pixel relationship between the reference and the target colour information. The colour reference library effectively solves the problem of choosing suitable reference images, colour error propagation, and the two-body problem in traditional colour-balancing methods. In addition, the proposed method is able to process images band by band, thus making it suitable to cope with multispectral images with any number of bands. Experimental results show that the proposed approach is feasible and performs better compared with the traditional ones.

2. Methods

The proposed method contains two parts: the establishment of a colour reference library and the colour-balancing method based on it. Unlike traditional methods, the proposed approach based on the colour reference library seems to be complicated, whereas in fact it is simple and practicable.

2.1. *Colour reference library*

Remote-sensing imagery is a reflection of the spectral reflectance characteristics of ground objects classified as natural features and man-made objects. The annual periodicity of the natural features indicates that the spectral reflectance characteristic also has a trait of cyclic variation, whereas the spectral reflectance characteristics of man-made objects are stable when there is no change. Thus, it can be assumed that no difference exists in the spectral reflectance characteristics between different images acquired at the same place and the same season, that is, the images should have the same colour. Then, the existing image data sets with the colour information that is visually appealing and consistent with the human visual perception can be selected as

the reference data to provide the colour reference information for images acquired at the same place and the same season. The colour reference library is a tool to organize and manage these data. It is worth noting that it is not the image data itself but the colour and related information extracted from it that are saved in the library. The reason will be explained in Section 2.1.2.

2.1.1. *Data source*

Big mosaic data set is becoming an increasingly significant data source for research and applications in the remote-sensing society (Zhou 2015). A growing number of mosaic products has been produced, whose quality is good with the characteristics of appropriate contrast, rich information, and clear texture. Many of them are produced for illustrative use only. Their colour information is visually appealing, seamless, and consistent with human visual perception, which is obtained by the work of human interaction on colour from experienced technical staff. Hence, the mosaic data, which are good-looking, seamless, and consistent with the human visual perception, can be chosen as the reference image.

Besides the mosaic image, other images with the colour information consistent with human visual perception can be selected as the reference data. Specifically, the orthorectified imagery of Landsat-8, which is open access, has a large coverage area and a short revisit period. Therefore, it is easy to use Landsat-8 data to obtain the colour reference of a large area after the work of human interaction on colour, which enriches the source of the reference data.

It is obvious to find that the criterion of selecting reference images providing the colour reference information is subjective. In fact, it is impractical to evaluate the quality of image colour by quantitative indices only, and a good-looking image is generally determined by human experience. Moreover, most of the state-of-the-art objective image quality assessment methods have been developed to leverage known characteristics of the human visual system (Wang et al. 2004), which means that subjective assessment is the decisive and ultimate quality measurement (Gu et al. 2015). With the help of subjective assessment, extra objective measurement is not needed in selecting suitable reference images in this article. Hence, the subjective judgment of human plays a key role in producing a visually appealing mosaic imagery. It can be inferred that the existing good-looking mosaic product generated by the experienced technical staff is the preferable reference data for the colour-balancing process. The reuse of existing data can effectively avoid the repetitive work of human interaction on colour for the images obtained in the same area and season, by which the processing efficiency of the colour-balancing method can be improved.

2.1.2. *The organization and storage of data*

The data source is organized according to the factors of geographical coverage, acquisition time, and spatial resolution. Specifically, the geographical coverage is divided into grids by latitude and longitude lines, each of which is numbered with a certain difference in latitude and longitude. When the geographical range of data source falls into the ith grid, the data source is labelled by G_i. The images are then classified by acquisition time, which is divided into four seasons (spring, summer, autumn, and winter) with the label of T_i. Finally, the images are sorted by spatial resolution marked

by R_i. After carrying out the classification mentioned above, each data source is labelled by $G_i - T_i - R_i$.

In most cases, mosaic data set has a wide geographic coverage, which indicates that a large memory space is needed for storage. Therefore, if the mosaic image itself is stored in the colour reference library, the memory space occupied by the library will be extremely large, which will restrict the scope of application of the library. Besides, the product of mosaic images in many data-producing agencies is usually not free. If the image itself is stored in the colour reference library, it is should be paid when the colour reference library is needed to copy from one agency to another, which goes against the wide use of the library. In order to solve this problem, it is not the image data itself but the colour and related information extracted from it that are saved in the library. The colour information includes mean and variance of the image, whereas the related information consists of thumbnail, acquisition time, and geographic information of the image (see Figure 1).

Because of the uneven distribution of ground objects in the image, different colours are distributed from area to area, which indicates that the mean and variance of the whole image cannot reflect the colour feature of the local areas. Thus, the algorithm of mean-shift colour segmentation (Comaniciu and Meer 2002) is applied in this article. Compared with other algorithms such as expectation maximization (EM) (Tai, Jia, and Tang 2005), mean-shift performs better in allowing unsupervised applications and improving the processing efficiency (Oliveira, Sappa, and Santos 2015). The image is segmented with the mean-shift colour segmentation algorithm, and a region fusion algorithm (Christoudias 2002) is used to guide image segmentation with edge information. A shape file is then created to record the edge information of the segmented regions (see Figure 2(*a*,*b*)). Therefore, the mean and variance of the image are computed region by region according to the segmentation information in the shape file. The mean and variance values in the regions and their corresponding shape files are treated as colour information to be stored in the colour reference library.

Since it is the colour information rather than the image itself that is stored in the colour reference library, the storage of memory is greatly reduced and the library is portable, that is, the colour reference library can be easily transferred among different agencies without limitations, which will greatly improve the flexibility and application range of the colour reference library. Moreover, the library can be updated with new data. The wider the geographical coverage of the library is, the wider the applicability of the library may become.

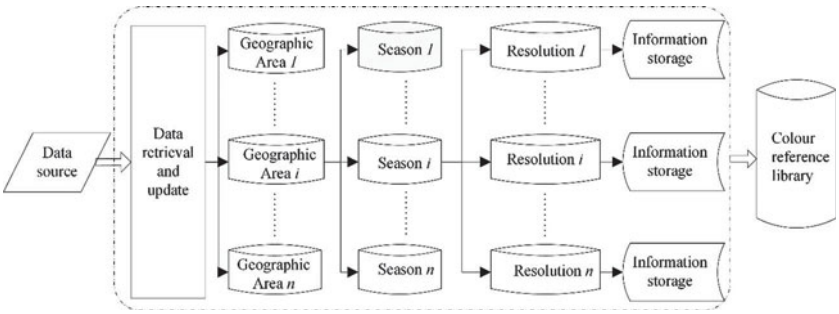

Figure 1. Organization chart of the colour reference library.

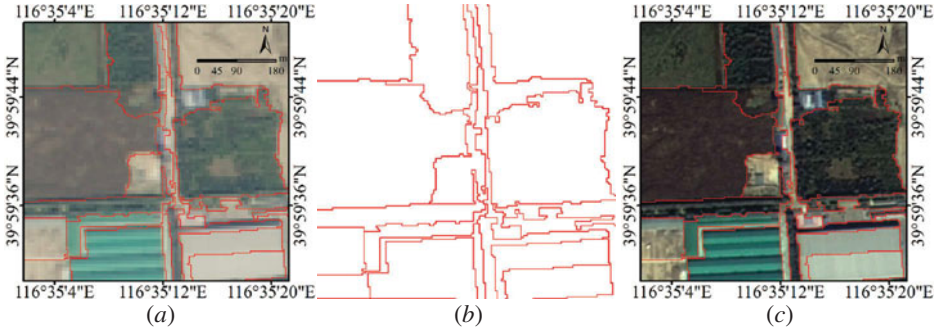

Figure 2. Example of segmentation of the reference data and the corresponding target image. (*a*) Segmentation result of the reference data with the mean-shift algorithm; (*b*) shape file recording the segmentation information of reference data; and (*c*) segmentation result of the target image with the shape file.

2.2. *Colour-balancing method based on a colour reference library*

The proposed method, which can automatically select suitable reference colour information for the target image and adaptively balance the colour, is specified in the following sections.

2.2.1. *Automatic selection of reference data*

Similar to the organization of the reference images described in Section 2.1.2, the factors of geographical coverage, acquisition time, and spatial resolution are also extracted from the target images. According to the factors, the target data source is labelled by $G_i^{'} - T_i^{'} - R_i^{'}$, by which the reference data with the same geographic coverage, the same acquisition season, and the closest spatial resolution with the target images is retrieved and selected in the colour reference library (see Figure 1). Note that the resolution of the reference data and that of the target image need not necessarily be the same.

It is worth noting that the target and reference data may come from different sensors in the proposed method. The reasons are as follows. On the one hand, display devices can only show the image with 8 bits. Generally, existing mosaic images selected to provide the reference colour information in the colour reference library are the production with 8 bits, and the target images are compressed to 8 bits in the preprocessing step before colour-balancing in this article. On the other hand, the colour information of an 8-bit image shown in the display device is the direct presentation of the digital number (DN) values of the image, that is, the same colour information shown in the display device corresponds to the same DN values of the images even from different sensors. It can be inferred that images from different sensors of the same ground object should have the same colour information after being compressed to 8 bits. Therefore, the reference data from different sensors can be selected in the proposed method.

2.2.2. *Standard regression model and colour information statistics*

It is known that colour-balancing methods can be divided into non-linear correction and linear correction according to different adjustment approaches. Linear correction

assumes that a linear transformation relationship exists between the target image and the reference image. In order to measure the linear transformation relationship, a number of linear regression models have been created. As mentioned above, it is the colour information, which is composed of the mean and variance values, rather than the image itself that is stored in the colour reference library. Under such situation, the standard regression model using mean and variance value only is adopted in this article to build the linear regression model between the reference information and the target images. Although the standard regression model is traditional, it is one of the best choices for the proposed method according to the circumstance mentioned above. In the standard regression model, the linear function is obtained as follows:

$$T_{\text{res}} = C_1 \times T_{\text{tar}} + C_2, \tag{1}$$

$$C_1 = \frac{\sigma_{\text{ref}}^2}{\sigma_{\text{tar}}^2}, \tag{2}$$

$$C_2 = \mu_{\text{ref}} - C_1 \times \mu_{\text{tar}}, \tag{3}$$

where T_{tar} is the pixel value of the target image, T_{res} is the colour-balancing result of T_{tar}, C_1 and C_2 are the linear coefficients, σ_{ref}^2 is the variance of the reference data, σ_{tar}^2 is the variance of the target image, μ_{ref} is the mean value of the reference data and μ_{tar} is the mean value of the target image.

It can be inferred that for building the standard regression model, the mean, variance value of reference data, and the corresponding value of the target image are needed.

As mentioned above, the reference data acquired from the colour reference library consists of the colour information, which is composed of the mean, variance values, and the shape file recording the segmentation information.

As described in Section 2.1.2, the mean and variance values stored in the colour reference library were extracted from the reference image region by region according to the segmentation information in the shape file. To derive the corresponding relationship between the target images and the reference data, the mean and variance value in the target images should also be calculated region by region according to the segmentation information in the shape file. It is worth noting that the shape file records the segmentation information of the reference data, and it may not be matching with the real situation of the target image. However, the purpose of the colour-balancing method proposed in this article is to create visually appealing satellite image mosaics for illustrative use only. Hence, the use of the shape file of the reference data to segment the target images is acceptable.

With the help of the corresponding mean and variance value between the reference data and target images, the linear coefficients can be calculated by Equations (2)–(3) region by region. If there are N corresponding regions between the reference and target data, N pairs of linear coefficients will be created. In order to obtain a smooth colour-balancing result, each pair of linear coefficients is weighted by a colour influence mask (Oliveira, Sappa, and Santos 2011; Ly et al. 2015).

2.2.3. *Colour influence mask and colour-balancing process*

A colour influence mask (CIM) measures the similarity of each pixel of the image and the mean value of each region (Oliveira, Sappa, and Santos 2011; Ly et al. 2015). The CIM of a region k with the mean colour μ^k is generated as follows.

(1) The euclidean distance (ED) between every pixel of the target image and the mean value of region k in the target image is calculated in the CIE $L^*a^*b^*$ (CIELAB) colour space. Since the CIELAB colour space can only address images with three bands, bands such as red, green, and blue are selected to calculate the ED in cases when more bands exist in the image.

$$d^k = \left\| T_i - \mu^k \right\|, \tag{4}$$

where T_i is the value of one pixel in the target image, μ^k is the mean value of the region k, and d^k is the ED between the pixel value and the region k.

(2) The distance p is introduced to normalize the maximum of d, which varies among different regions. When the ED is very small, that is, the colour of the pixel is close to the mean value of the region, the distance $p$approaches 1 and 0 vice versa.

$$p^k = 1 - \frac{d^k}{\max(d^k)}, \tag{5}$$

where p^k is the normalized value of d^k.

(3) The CIM is calculated by Equation (6):

$$M^k = e^{a(p^k)^b}, \tag{6}$$

where M^k is the CIM of region k under the ED of d^k; and a and b are tuning parameters. In this article, $a = 10$ and $b = 2$.

The example of CIM is shown in Figure 3. Then the result can be generated according to Equation (7) by combining the linear coefficients of N regions weighted by N CIMs.

Figure 3. Two examples of colour influence mask (CIM) in regions 1 and 2 of image (*a*), where (*a*) is the segmentation result of the target image, (*b*) is the CIM in region 1, and (*c*) is the CIM in region 2. If the value of a pixel is close to the mean value of the particular region, the CIM value of the pixel in that region is high even though it is not within the region.

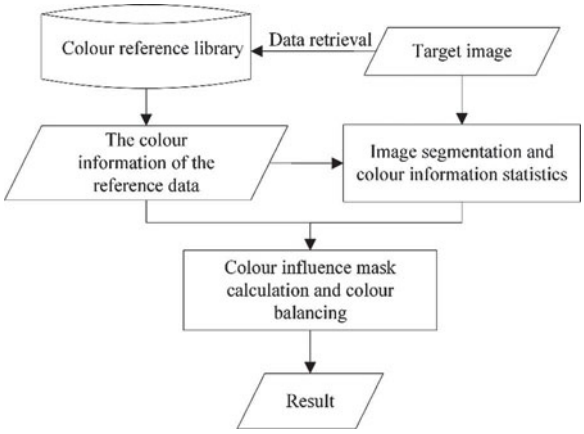

Figure 4. Flow chart of the colour-balancing method based on a colour reference library.

$$T_{\text{res}} = \frac{\sum_{k=1}^{N} (C_1^k \times T_{\text{tar}} + C_2^k) \times M^k}{\sum_{k=1}^{N} M^k}, \tag{7}$$

where C_1^k and C_2^k are the linear coefficients of the region k, and M^k is the CIM between the pixel T_{tar} and the region k.

The flow chart of the colour-balancing method based on a colour reference library is shown in Figure 4.

2.3. *Validation of the results*

To evaluate the performance of the results in an objective way, root mean square error (RMSE), ED, and entropy are applied. Unlike traditional methods calculating the RMSE and ED in the RGB colour space, CIELAB colour space was adopted to evaluate the results quantitatively. CIELAB colour space, one of the most comprehensive colour models describing colours in human vision, is an approximately uniform colour space independent of display devices (Hill, Roger, and Vorhagen 1997).

2.3.1. *Root mean square error*

RMSE is a commonly applied evaluation index describing the difference between two corresponding images. A small value indicates a close relationship between the images (Helmer and Ruefenacht 2005).

$$R = \sqrt{\frac{\sum_{i=1}^{n} (T_{\text{ref}_i} - T_{\text{cor}_i})^2}{n}}, \tag{8}$$

where R is the RMSE value, n is the pixel number, T_{ref_i} is the grey value of the ith pixel in the reference image, and T_{cor_i} is the corresponding calibrated value.

2.3.2. *Euclidean distance*

ED was also adopted to measure the difference between two corresponding images. A small value indicates a close relationship in information between images.

$$E = \frac{\sum_{i=1}^{n} \sqrt{(L_{\mathrm{ref}_i} - L_{\mathrm{cor}_i})^2 + (a_{\mathrm{ref}_i} - a_{\mathrm{cor}_i})^2 + (b_{\mathrm{ref}_i} - b_{\mathrm{cor}_i})^2}}{n}, \tag{9}$$

where E is the value of ED, and $(L_{\mathrm{ref}_i}, a_{\mathrm{ref}_i}, b_{\mathrm{ref}_i})$ and $(L_{\mathrm{cor}_i}, a_{\mathrm{cor}_i}, b_{\mathrm{cor}_i})$ are the ith pixel value between the reference and corresponding images in the CIELAB space, respectively.

2.3.3. *Entropy*

Entropy is an index of stating the richness of information of the image, which is calculated in RGB colour space since it has little relationship with human vision. A high value indicates that the image is rich in information.

$$H = -\sum_{i=0}^{L-1} P_i \times \log_2(P_i), \tag{10}$$

where H is the value of entropy, P_i is the probability of value i, and L represents the grey level.

3. Results and analysis

3.1. *Experiment data*

Images from Zi-Yuan 3 (ZY-3) (Zhang et al. 2015a) and Gao-Fen 1(GF-1) (Zhang et al. 2015b) satellites of China were used as experimental data. Three data sets were selected for experimentation and analysis. The first data set includes 17 fused images of ZY-3 covering Beijing of China with the spatial resolution of 2.1 m. The size of the images is around 40000 × 30000 pixels. The acquisition time of the images was mainly distributed from August to October 2013, and a small number of images was acquired in May 2013 and January 2014. The second data set consists of 27 fused images of ZY-3 and two fused images of GF-1 in Jiangsu, China, with the size around 35000 × 30000 pixels. The majority of the acquisition time was distributed from August to November 2013, and a small number of images was acquired in April 2012, May 2013, and January 2014. The spatial resolution here too was 2.1 m. The third data set includes six fused images of ZY-3 in Shanxi, China, with the spatial resolution of 2.1 m. The size of the images is around 34000 × 26000 pixels. The acquisition time of the images was distributed in September 2012 and in May 2013. Although the proposed method can address images with any number of bands, three bands of the image were selected for the experiment, as display devices can only show three bands. The red, green, and blue bands were selected in the first two data sets, and the near-infrared, red, and green bands were selected in the third data set, since both of them are the common band combination in satellite imagery application. All experimental data were stretched to 8 bits. Each experiment data set was ortho-rectified to the same resolution with control points and the digital elevation model, and the RMSE was less than 0.5 pixel. The World Geodetic System (WGS) 84

data with the longitude and latitude coordinates were used in all images (Canty, Nielsen, and Schmidt 2004; Hu et al. 2011; Schroeder et al. 2006).

3.2. *Results*

The mosaic product of the experimental data was generated in the previous process, which can be selected as the reference data. The first two mosaic data are composed of ZY-3 and GF-1 satellite imageries; the third mosaic data include Landsat 8 OLI images. In the proposed method, the colour reference library was first updated with the mosaic data, which were then chosen as the reference for subsequent processing. Moreover, to further evaluate the proposed method, contrast experiments were conducted in this article. To exclude the influences of different reference data for different colour-balancing methods, the same reference data are used in all of the experiments. Under this condition, the methods that can take the existing image as the reference data are selected in this article. Hence, the multiple auto-adapting colour-balancing method (MACB) (Zhou 2015), the histogram match method (HISMAT) (Helmer and Ruefenacht 2005), the Wallis transform method (Wallis) (Sun and Zhang 2008), the I-SFA method (Zhang, Wu, and Du 2014), and the IR-MAD method (Canty and Nielsen 2008) were selected to compare with the proposed method, which is named the colour-balancing method based on a colour reference library (CBCRL). The same mosaic data providing the reference colour information for the proposed method were adopted as the reference data for the comparison methods. The correction results of each method were inlaid with the same mosaic method, as is shown in Figures 5–10, from which 'Tar' is short for the target image, 'Ref' is short for the reference data, 'CBCRL' represents the mosaic result of the proposed method, 'MACB', 'HISMAT', 'I-SFA', and 'IR-MAD' stand for the mosaic results of different methods, respectively.

3.2.1. *Visual assessments*

Figures 5, 7, and 9 are the overall thumbnails of the experiment data sets, Figures 6 and 8 are the details of the areas marked by a red box in Figures 5 and 7, and Figure 10 is the detail of the areas marked by a green box in Figure 9. As is shown in the representative areas marked by the yellow circle in (*a*) and (*b*) of Figures 5–10, a big colour difference exists not only between the images in each experiment data set but also between the target image and the reference image. From Figures 5, 7, and 9, it can be inferred that the colour differences in the original experiment data sets are reduced in the results of different methods to varying degrees. Taking Figure 7 as an example, it is obvious that there exist colour differences in the areas marked by the yellow circle in (*e*)–(*h*). For the results in (*c*) and (*d*), colour differences are eliminated, between which the colour information of the former is closer to the reference. Similar conclusions can be gained from Figures 5 and 9, although it is less obvious owing to the size of the picture shown in the article. To observe the differences among the results of different methods more clearly, three details were selected from the data sets, respectively, in Figures 6, 8, and 10, from which it is obvious to find that colour differences still exist in (*d*)–(*h*), whereas the result of the proposed method in (*c*) is seamless with the colour close to the reference. In general, it is obvious that CBCRL, whose results are seamless with the colour close to the reference, outperforms the other methods, and colour differences

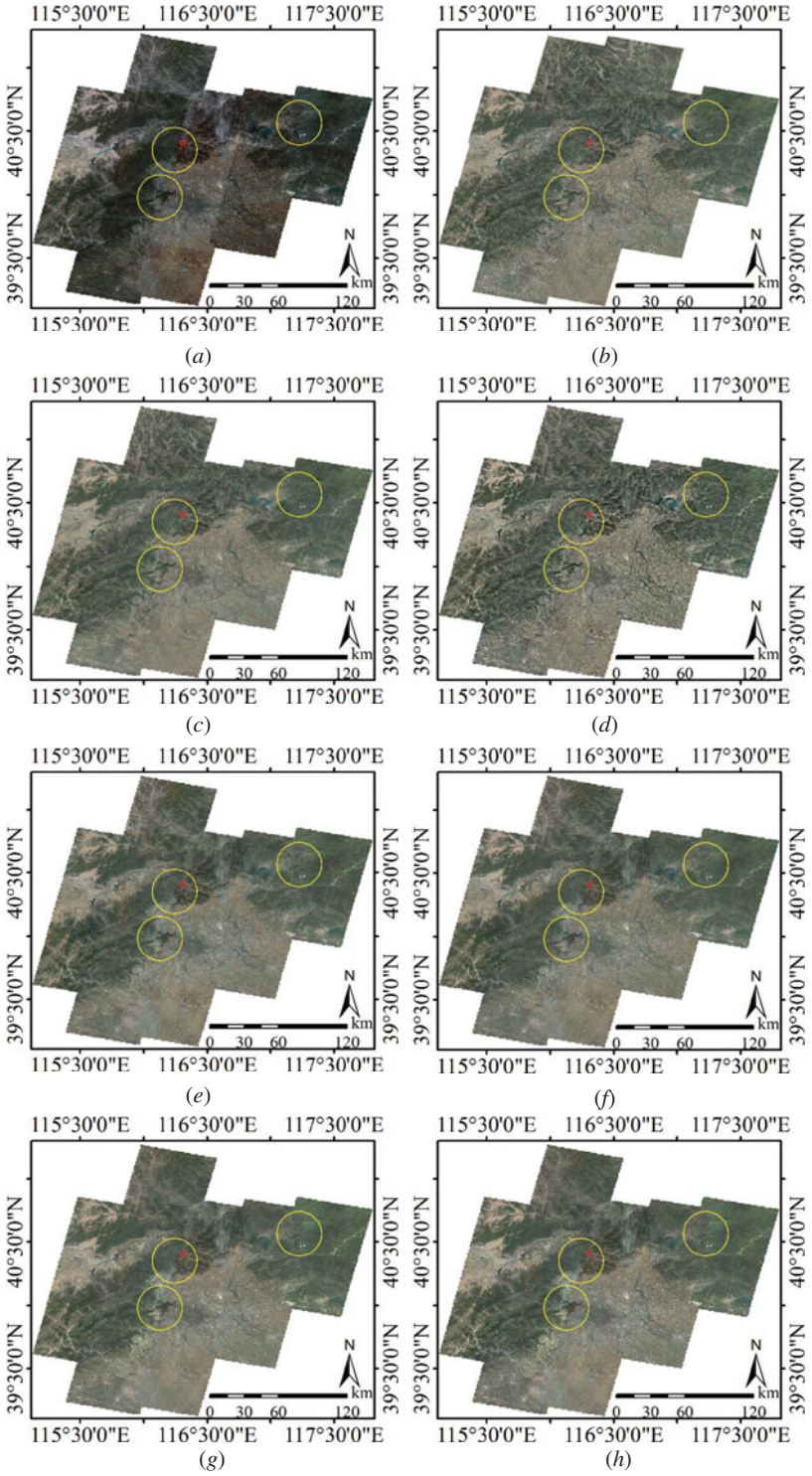

Figure 5. Thumbnail results of the first data set under different methods: (*a*) Tar; (*b*) Ref; (*c*) CBCRL; (*d*) MACB; (*e*) HISMAT; (*f*) Wallis; (*g*) I-SFA; and (*h*) IR-MAD.

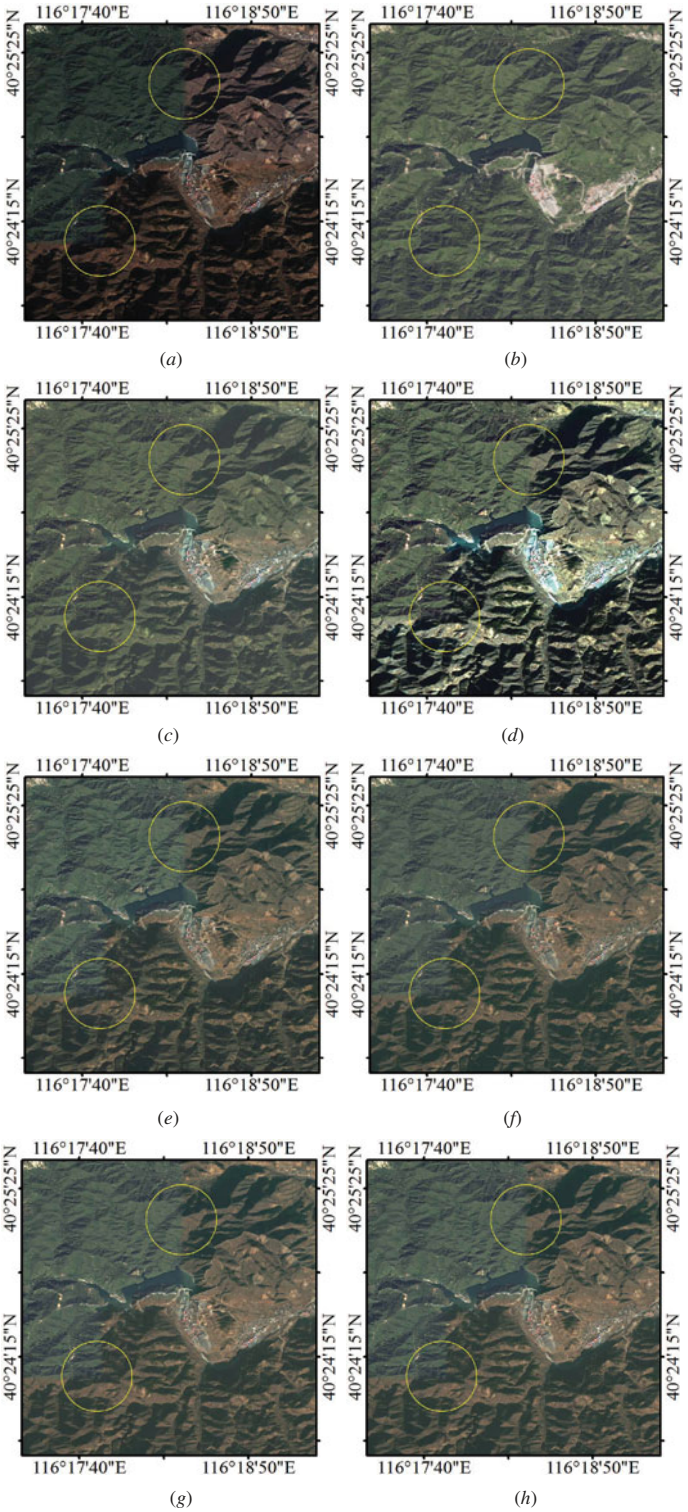

Figure 6. Detailed results of the first data set under different methods: (*a*) Tar; (*b*) Ref; (*c*) CBCRL; (*d*) MACB; (*e*) HISMAT; (*f*) Wallis; (*g*) I-SFA; and (*h*) IR-MAD.

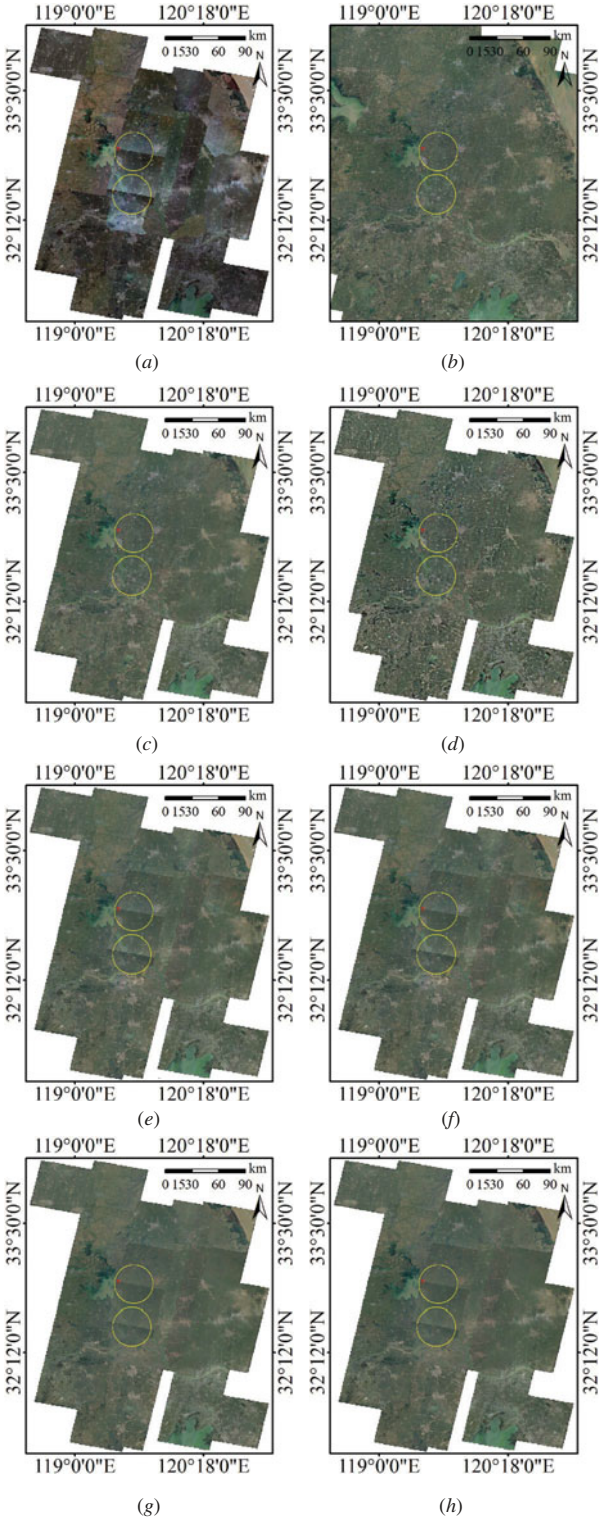

Figure 7. Thumbnail results of the second data set under different methods: (*a*) Tar; (*b*) Ref; (*c*) CBCRL; (*d*) MACB; (*e*) HISMAT; (*f*) Wallis; (*g*) I-SFA; and (*h*) IR-MAD.

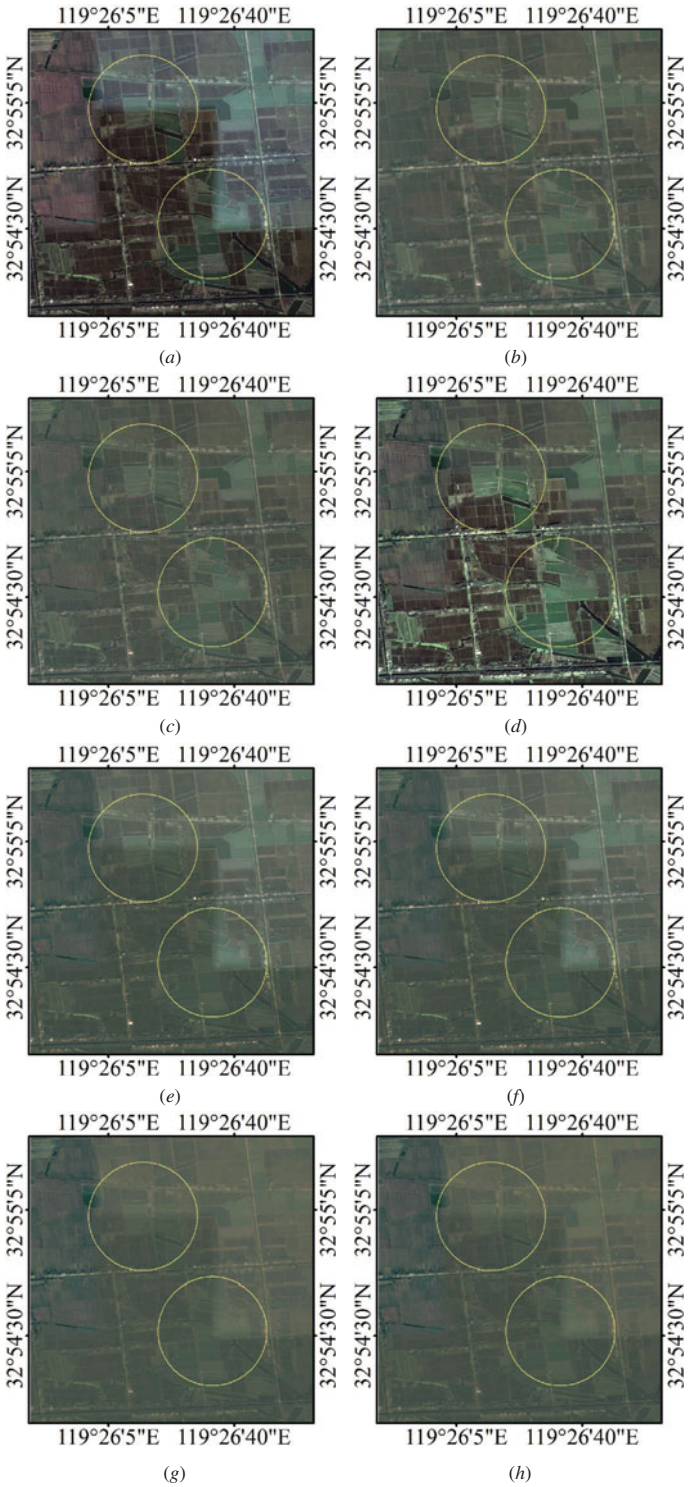

Figure 8. Detailed results of the second data set under different methods: (*a*) Tar; (*b*) Ref; (*c*) CBCRL; (*d*) MACB; (*e*) HISMAT; (*f*) Wallis; (*g*) I-SFA; and (*h*) IR-MAD.

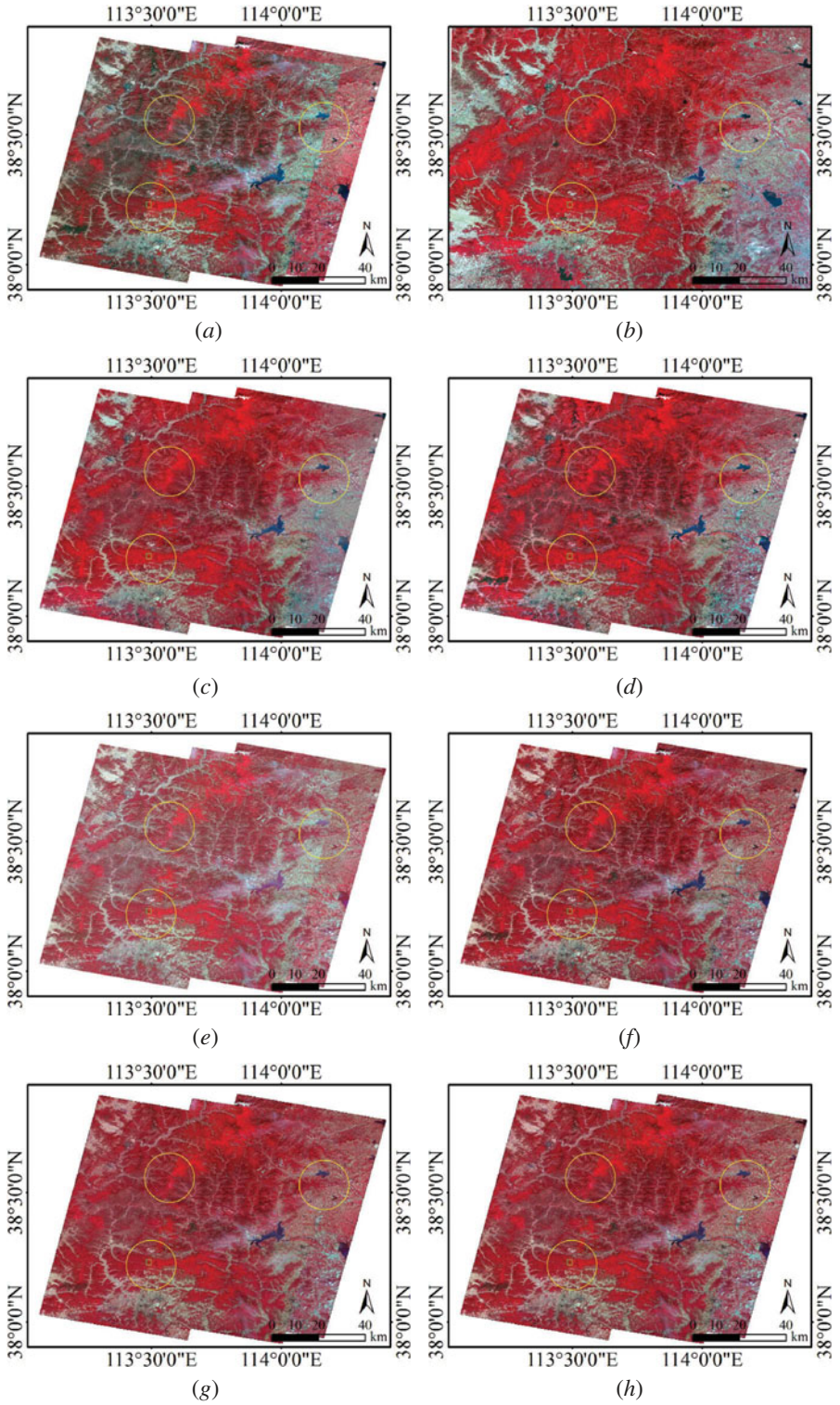

Figure 9. Thumbnail results of the third data set under different methods: (*a*) Tar; (*b*) Ref; (*c*)CBCRL; (*d*) MACB; (*e*) HISMAT; (*f*) Wallis; (*g*) I-SFA; and (*h*) IR-MAD.

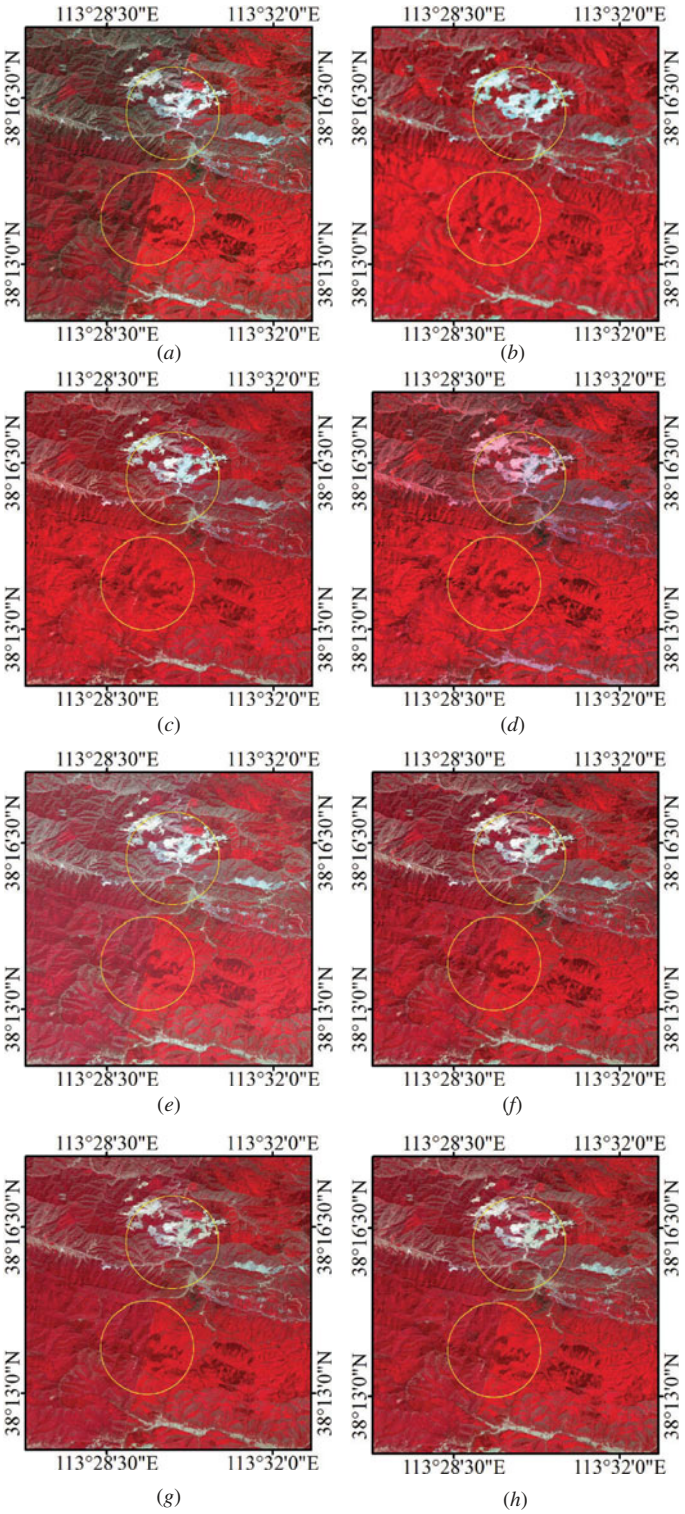

Figure 10. Detailed results of the third data set under different methods: (*a*) Tar; (*b*) Ref; (*c*) CBCRL; (*d*) MACB; (*e*) HISMAT; (*f*) Wallis; (*g*) I-SFA; and (*h*) IR-MAD.

still exist in the results of the other methods. The above results demonstrate that the proposed method performs the best compared with the other methods in this article, and it can eliminate the difference in target images and remove the difference between the reference data and the target images. Since the reference data are selected from the existing mosaic data, which are visually appealing, seamless, and consistent with the human visual perception, the colour-balancing results are also good-looking without requiring the further repetitive work of human interaction on colour, which speeds up the process of the colour-balancing method.

3.2.2. *Statistical analysis*

The statistical results between the reference data and the resulting image are shown in Tables 1–3. The columns corresponding to the different methods in the table represent the evaluation results of the images processed by the method; in addition, the numbers marked as underlined in each row are the best values among the different methods.

It can be inferred from Tables 1–3 that for RMSE and ED, the statistical results of the colour-balanced images are smaller than that of the target image, that is, the colour differences between the reference data and the target images are reduced with the help of colour-balancing methods. It is obvious to find that CBCRL yields the best result in RMSE and ED in the three data sets, whereas MACB is less effective in the first two data sets and HISMAT is less effective in the third one. In other words, the result of CBCRL has the closest colour to the reference data; however, colour distortions in

Table 1. The evaluation comparison table of the results of the first experiment data set under different methods (the underlined numbers in each row are the best value among the different methods).

	Method / Band	Tar	CBCRL	MACB	HISMAT	Wallis	I-SFA	IR-MAD
RMSE	1	0.8552	0.5343	0.8347	0.6973	0.6856	0.7039	0.7201
	2	0.8548	0.3754	0.6866	0.4632	0.4650	0.4965	0.5027
	3	2.8241	1.2781	2.1727	1.4761	1.4907	1.5216	1.5548
ED		1.6169	0.6298	1.1322	0.7811	0.7836	0.7881	0.8018
Entropy	1	6.9587	7.0838	7.4505	6.7376	6.8265	6.7783	6.7810
	2	6.8309	6.9676	7.4446	6.5911	6.5792	6.5766	6.5866
	3	6.6021	6.7077	7.2661	6.3316	6.2693	6.2966	6.3052

Table 2. The evaluation comparison table of the results of the second experiment data set under different methods (the underlined numbers in each row are the best value among the different methods).

	Method / Band	Tar	CBCRL	MACB	HISMAT	Wallis	I-SFA	IR-MAD
RMSE	1	1.1569	0.5232	0.9987	0.6996	0.7078	0.6713	0.6694
	2	1.0838	0.2534	0.7984	0.3977	0.4008	0.3681	0.3715
	3	2.1140	0.7808	1.9933	0.9942	1.0031	0.9468	0.9624
ED		1.4501	0.3737	1.0648	0.5585	0.5660	0.5290	0.5326
Entropy	1	6.9124	7.0992	7.2164	6.4799	6.4841	6.3637	6.3812
	2	6.7269	6.7671	7.2576	6.1662	6.1673	5.9458	5.9663
	3	6.5631	6.4743	7.0384	5.8146	5.8169	5.5553	5.5801

Table 3. The evaluation comparison table of the results of the third experiment data set under different methods (the underlined numbers in each row are the best value among the different methods).

	Method / Band	Tar	CBCRL	MACB	HISMAT	Wallis	I-SFA	IR-MAD
RMSE	1	5.7941	1.9357	3.8764	4.3269	3.4827	3.4441	3.4687
	2	3.5206	1.3658	2.6154	2.5936	2.2894	2.2246	2.2606
	3	2.1100	1.2886	2.5609	2.9138	1.7779	1.6772	1.6822
ED		3.5912	1.5610	2.3909	2. 8836	2.1134	2.0436	2.0656
Entropy	1	6.7001	6.9870	7.3986	6.0469	6.5604	6.3450	6.4379
	2	7.1678	7.1744	7.1885	6.7437	6.9084	6.8744	6.8750
	3	6.8818	6.9576	7.1327	6.3140	6.8357	6.6140	6.6833

different degrees exist in the other results, which are consistent with the above-mentioned judgments. It can be found that the values of RMSE and ED in the third experiment are bigger than those in the first two data sets. The reason for this situation is that the big difference of spatial resolution between the reference and target data sets goes against the precision extraction of the corresponding points to calculate the values of RMSE and ED, which leads to the bigger value in the third experiment. The result of MACB has the biggest value in entropy, which is greater than that of the origin target image, which means that the information of the result of MACB is enhanced. As a result of the enhancement, big colour distortions still exist in the result of MACB compared with the other methods. However, the entropy value of the result of CBCRL is close to the target image and is better than the other results, indicating that the proposed CBCRL method performs better in information retaining. In general, the proposed method outperforms the other methods in both colour difference reducing and information retaining.

4. Discussion

A colour-balancing method has been proposed in this article to eliminate the effect of colour difference between different images for seamless image mosaic based on the colour reference library. Unlike the uncertainty standard of choosing the reference image in traditional methods, the suitable reference data can be extracted from the colour reference library storing colour information of the existing mosaic imagery, which is visually appealing and consistent with human visual perception in the proposed method. The colour information with the same geographic coverage, acquisition season, and the closest spatial resolution as the target images can be provided as the reference for the proposed approach, by which the problem of choosing the reference images in traditional methods can be solved.

Besides, with the help of the colour reference library, the proposed method can effectively avoid the two-body problem, which is a big obstacle to traditional methods. For most of the existing methods, only a single pair of the target images can be processed at a time. Therefore, in most cases, the target images will be proceeded sequentially, which will slow down the process and thereby introduce the risk of colour error propagation. However, for the proposed method, the selected reference

data have the same geographic coverage as the target images, that is, each target image has its own geography-related reference data. Hence, the target images can be corrected independently and no sequential relationship exists among the processing procedures, thus avoiding the two-body problem effectively and contributing to parallel processing.

Moreover, the processes of sensor calibration and atmospheric correction are not needed in the proposed method for the following reasons. First, the reference data used in this article are the existing mosaic image data sets, whose colour information is visually appealing, seamless, and consistent with human visual perception. Therefore, the processes of sensor calibration and atmospheric correction are not necessary for the existing mosaic images, their production processes are not taken into consideration in the proposed method. Moreover, the process steps of sensor calibration and atmospheric correction are not essential for the target images. The purpose of the proposed method is to adjust the colour information of the target images to be the same with the reference colour information for visually appealing and seamless image mosaicking. If the target images were first processed by sensor calibration and atmospheric correction, the intermediate result also needs to be adjusted to be the same with the reference colour information, indicating that sensor calibration and atmospheric correction are not necessary. Hence, sensor calibration and atmospheric correction are not needed in the proposed method.

In addition, images are generally considered as a whole in the calculation process of colour correction in traditional approaches. In other words, only one transformation model exists in an image, which may result in neglecting the locality and inhomogeneity of the ground objects' distribution. The strategy of colour segmentation is applied in the proposed method, which can reflect the colour distribution of the images and perform better than the colour information extracted from the image as a whole. Figures 5–10 demonstrate that the proposed method has a better performance than the others discussed in this article, which can eliminate the difference in target images and remove the difference between the reference data and the target images. Tables 1–3 also demonstrate that the proposed method outperforms the other methods in both colour difference reducing and information retaining.

As mentioned above, the colour reference library in this article, developed from the existing mosaic data, is of great significance in the proposed colour-balancing method. The repetitive work of human interaction on colour for the images obtained in the same area and acquisition season as the existing data can be avoided by reusing the existing data. In this way, the process speed of the colour-balancing method can be improved. The storage of memory is greatly reduced and the library is portable since the colour information rather than the image itself is stored in the colour reference library. Moreover, the library can be updated with new data. The wider the geographical coverage of the library is, the wider the applicability of the library may become.

For further study, more suitable existing images are needed to extend the geographical coverage of the colour reference library to improve its applicability. Besides, in the present work, the values of mean and variance are stored as the reference colour information in the colour reference library, and some other more suitable indices may be extracted in a future work.

5. Conclusions

In order to eliminate the effect of colour difference between different images for visually appealing and seamless image mosaic, a novel colour-balancing method for satellite imagery based on the colour reference library is proposed in this article. The colour reference library, with the ability to collect the existing image, is introduced to improve data storage and utilization, through which the problem of selecting the reference can be solved, and colour error propagation and the two-body problem in traditional colour-balancing methods can be avoided. The storage of memory is greatly reduced and the library is portable due to the storage of colour information rather than the image itself. The advantages of the colour reference library are fully used in the proposed method by first selecting the suitable colour information as the reference and then developing the pixel-to-pixel relationship between the colour information of the reference data and that of the target image. The proposed colour-balancing method, making full use of the advantages of the colour reference library, can select reference colour data automatically and process the target image adaptively. Through band-by-band processing, the proposed method can be used for processing multispectral images with any number of bands if the corresponding reference bands' information is stored in the library. Since the colour of the images corrected by the proposed method is very close to that of the reference data, which are consistent with human vision habit, the extra work of human interaction on colour is not required, which is time-saving. The experimental results demonstrate that the proposed method is feasible and efficient.

Acknowledgements

This work was supported in part by the National Natural Science Foundation of China with project number 41322010 and 41571434, the National High Technology Research and Development Program of China with project number 2013AA12A401 and 2013AA0630905.

Disclosure statement

No potential conflict of interest was reported by the authors.

Funding

This work was supported by the National Natural Science Foundation of China [41322010]; [41571434]; National the National High Technology Research and Development Program of China [2013AA12A401]; [2013AA0630905].

References

Canty, M. J., and A. A. Nielsen. 2008. "Automatic Radiometric Normalization of Multitemporal Satellite Imagery with the Iteratively Re-Weighted MAD Transformation." *Remote Sensing of Environment* 112 (3): 1025–1036. doi:10.1016/j.rse.2007.07.013.

Canty, M. J., A. A. Nielsen, and M. Schmidt. 2004. "Automatic Radiometric Normalization of Multitemporal Satellite Imagery." *Remote Sensing of Environment* 91 (3–4): 441–451. doi:10.1016/j.rse.2003.10.024.

Chen, C., Z. Chen, M. Li, Y. Liu, L. Cheng, and Y. Ren. 2014. "Parallel Relative Radiometric Normalisation for Remote Sensing Image Mosaics." *Computers & Geosciences* 73: 28–36. doi:10.1016/j.cageo.2014.08.007.

Chen, X., L. Vierling, and D. Deering. 2005. "A Simple and Effective Radiometric Correction Method to Improve Landscape Change Detection across Sensors and across Time." *Remote Sensing of Environment* 98 (1): 63–79. doi:10.1016/j.rse.2005.05.021.

Christoudias, C. M. 2002. "Synergism in Low Level Vision." *International Conference on Pattern Recognition* 4: 150–155. doi:10.1109/ICPR.2002.1047421.

Cihlar, J., B. Guindon, J. Beaubien, R. Latifovic, D. Peddle, M. Wulder, R. Fernandes, and J. Kerr. 2003. "From Need to Product: A Methodology for Completing A Land Cover Map of Canada with Landsat Data." *Canadian Journal of Remote Sensing* 29 (2): 171–186. doi:10.5589/m02-090.

Comaniciu, D., and P. Meer. 2002. "Mean Shift: A Robust Approach toward Feature Space Analysis." *IEEE Transactions on Pattern Analysis and Machine Intelligence* 24 (5): 603–619. doi:10.1109/34.1000236.

Cresson, R., and N. Saint-Geours. 2015. "Natural Color Satellite Image Mosaicking Using Quadratic Programming in Decorrelated Color Space." *IEEE Journal of Selected Topics in Applied Earth Observations and Remote Sensing* 8 (8): 4151–4162. doi:10.1109/JSTARS.2015.2449233.

de Carvalho, O., R. Guimarães, N. Silva, A. Gillespie, R. Gomes, C. Silva, and A. de Carvalho. 2013. "Radiometric Normalization of Temporal Images Combining Automatic Detection of Pseudo-Invariant Features from the Distance and Similarity Spectral Measures, Density Scatterplot Analysis, and Robust Regression." *Remote Sensing* 5 (6): 2763–2794. doi:10.3390/rs5062763.

Du, Y., P. M. Teillet, and J. Cihlar. 2002. "Radiometric Normalization of Multitemporal High-Resolution Satellite Images with Quality Control for Land Cover Change Detection." *Remote Sensing of Environment* 82: 123–134. doi:10.1016/S0034-4257(02)00029-9.

Gu, K., G. Zhai, X. Yang, and W. Zhang. 2015. "Using Free Energy Principle for Blind Image Quality Assessment." *IEEE Transactions on Multimedia* 17 (1): 50–63. doi:10.1109/TMM.2014.2373812.

Helmer, E. H., and B. Ruefenacht. 2005. "Cloud-Free Satellite Image Mosaics with Regression Trees and Histogram Matching." *Photogrammetric Engineering & Remote Sensing* 71 (9): 1079–1089. doi:10.14358/PERS.71.9.1079.

Hill, B., T. Roger, and F. W. Vorhagen. 1997. "Comparative Analysis of the Quantization of Color Spaces on the Basis of the CIELAB Color-Difference Formula." *ACM Transactions on Graphics* 16 (2): 109–154. doi:10.1145/248210.248212.

Hu, Y., L. Liu, L. Liu, and Q. Jiao. 2011. "Comparison of Absolute and Relative Radiometric Normalization Use Landsat Time Series Images Yong." *MIPPR 2011: Remote Sensing Image Processing* 8006: 800616–800616–8. doi:10.1117/12.902076.

Ibrahim, M. T., R. Hafiz, M. M. Khan, and Y. Cho. 2015. "Automatic Selection of Color Reference Image for Panoramic Stitching." *Multimedia Systems* 1–14. doi:10.1007/s00530-015-0467-4.

Liu, J., X. Wang, M. Chen, S. Liu, Z. Shao, X. Zhou, and P. Liu. 2014. "Illumination and Contrast Balancing for Remote Sensing Images." *Remote Sensing* 6 (2): 1102–1123. doi:10.3390/rs6021102.

Ly, D. S., S. Beucher, M. Bilodeau, S. Persa, K. J. Damstra, R. Pot, and J. V. Rooy. 2015. "Automatic Color Correction: Region-Based Approach and Performance Evaluation Using Full Reference Metrics." *Journal of Electronic Imaging* 24 (6): 061207. doi:10.1117/1.JEI.24.6.061207.

Moran, M. S., R. D. Jackson, P. N. Slater, and P. M. Teillet. 1992. "Evaluation of Simplified Procedures for Retrieval of Land Surface Reflectance Factors from Satellite Sensor Output." *Remote Sensing of Environment* 41 (2–3): 169–184. doi:10.1016/0034-4257(92)90076-V.

Oliveira, M., A. D. Sappa, and V. Santos. 2011. "Unsupervised Local Color Correction for Coarsely Registered Images." Paper presented at the annual Conference for IEEE Computer Society of Computer Vision and Pattern Recognition, Colorado, June 201–208. doi:10.1109/CVPR.2011.5995658.

Oliveira, M., A. D. Sappa, and V. Santos. 2015. "A Probabilistic Approach for Color Correction in Image Mosaicking Applications." *IEEE Transactions on Image Processing* 24 (2): 508–523. doi:10.1109/TIP.2014.2375642.

Olthof, I., D. Pouliot, R. Fernandes, and R. Latifovic. 2005. "Landsat-7 ETM+ Radiometric Normalization Comparison for Northern Mapping Applications." *Remote Sensing of Environment* 95 (3): 388–398. doi:10.1016/j.rse.2004.06.024.

Paolini, L., F. Grings, J. A. Sobrino, J. C. Jiménez Muñoz, and H. Karszenbaum. 2006. "Radiometric Correction Effects in Landsat Multi-Date/Multi-Sensor Change Detection Studies." *International Journal of Remote Sensing* 27 (4): 685–704. doi:10.1080/01431160500183057.

Sadeghi, V., H. Ebadi, and F. F. Ahmadi. 2013. "A New Model for Automatic Normalization of Multitemporal Satellite Images Using Artificial Neural Network and Mathematical Methods." *Applied Mathematical Modelling* 37 (9): 6437–6445. doi:10.1016/j.apm.2013.01.006.

Schroeder, T. A., W. B. Cohen, C. Song, M. J. Canty, and Z. Yang. 2006. "Radiometric Correction of Multi-Temporal Landsat Data for Characterization of Early Successional Forest Patterns in Western Oregon." *Remote Sensing of Environment* 103 (1): 16–26. doi:10.1016/j.rse.2006.03.008.

Song, C., C. E. Woodcock, K. C. Seto, M. P. Lenney, and S. A. Macomber. 2001. "Classification and Change Detection Using Landsat TM Data : When and How to Correct Atmospheric Effects ?" *Remote Sensing of Environment* 75 (2): 230–244. doi:10.1016/S0034-4257(00)00169-3.

Sun, M., and J. Zhang. 2008. "Dodging Research for Digital Aerial Images." *The International Archives of the Photogrammetry, Remote Sensing and Spatial Information Sciences* XXXVII: Par:349–354.

Tai, Y. W., J. Jia, and C. K. Tang. 2005. "Local Color Transfer via Probabilistic Segmentation by Expectation-Maximization." Paper presented at the annual Conference for IEEE Computer Society of Computer Vision and Pattern Recognition, San Diego, June I(1) :747–754. doi:10.1109/CVPR.2005.215

Tsai, V. J.-D., and Y.-T. Huang. 2005. "Automated Image Mosaicking." *Journal of the Chinese Institute of Engineers* 28 (2): 329–340. doi:10.1080/02533839.2005.9670998.

Wang, J., Y. Ge, G. B. M. Heuvelink, C. Zhou, and D. Brus. 2012. "Effect of the Sampling Design of Ground Control Points on the Geometric Correction of Remotely Sensed Imagery." *International Journal of Applied Earth Observation and Geoinformation* 18: 91–100. doi:10.1016/j.jag.2012.01.001.

Wang, Z., A. C. Bovik, H. R. Sheikh, and E. P. Simoncelli. 2004. "Image Quality Assessment: From Error Visibility to Structural Similarity." *IEEE Transactions on Image Processing* 13 (4): 600–612. doi:10.1109/TIP.2003.819861.

Xu, W., and J. Mulligan. 2010. "Performance Evaluation of Color Correction Approaches for Automatic Multi-View Image and Video Stitching." Paper presented at the annual Conference for IEEE Computer Society of Computer Vision and Pattern Recognition, San Francisco, June 263–270. doi:10.1109/CVPR.2010.5540202.

Yang, X., and C. P. Lo. 2000. "Relative Radiometric Normalization Performance for Change Detection from Multi-Date Satellite Images." *Photogrammetric Engineering & Remote Sensing* 66: 967–980.

Zhang, L., C. Wu, and B. Du. 2014. "Automatic Radiometric Normalization for Multitemporal Remote Sensing Imagery With Iterative Slow Feature Analysis." *IEEE Transactions on Geoscience and Remote Sensing* 52 (10): 6141–6155. doi:10.1109/TGRS.2013.2295263.

Zhang, Y., Y. Wan, B. Wang, Y. Kang, and J. Xiong. 2015b. "Automatic Processing of Chinese Gf-1 Wide Field of View Images." *ISPRS - International Archives of the Photogrammetry, Remote Sensing and Spatial Information Sciences* XL-7/W3: 729–734. doi:10.5194/isprsarchives-XL-7-W3-729-2015.

Zhang, Y., M. Zheng, X. Xiong, and J. Xiong. 2015a. "Multistrip Bundle Block Adjustment of Zy-3 Satellite Imagery by Rigorous Sensor Model without Ground Control Point." *IEEE Geoscience & Remote Sensing Letters* 12 (4): 865–869. doi:10.1109/LGRS.2014.2365210.

Zhou, X. 2015. "Multiple Auto-Adapting Color Balancing for Large Number of Images." *ISPRS - International Archives of the Photogrammetry, Remote Sensing and Spatial Information Sciences* XL-7/W3: 735–742. doi:10.5194/isprsarchives-XL-7-W3-735-2015.